6th International Conference from "Scientific Computing to Computational Engineering"
6th IC-SCCE
Athens, 9-12 July, 2014

MONTE CARLO CALCULATIONS OF THE DETECTION SOLID ANGLE OF ELECTRONS EMITTED FROM SLOWLY DECAYING PROJECTILE ION AUGER STATES

S. Doukas[1], N. Angelinos[2], A. Kanellakopoulos[3], I. Madesis[2,4], A. Dimitriou[2,4], E.P. Benis5, and T.J.M. Zouros2,4

[1] Department of Material Science and Engineering, University of Ioannina, GR 45110 Ioannina, Greece
[2] Department of Physics, University of Crete, P.O.Box 2208, GR 71003 Heraklion, Greece
[3] Department of Physics, University of Athens, Zografou Campus, GR 15784 Athens, Greece
[4] Tandem Accelerator Laboratory, INP, NCSR Demokritos, GR 15310 Ag. Paraskevi, Greece
[5] Department of Physics, University of Ioannina, GR 45110 Ioannina, Greece

Keywords: Electron spectroscopy, Auger decay, Zero-degree spectroscopy, Metastable states, SIMION simulations, Monte Carlo type calculations, highly charged ions, ion-atom collisions

Abstract. *The long life times of the 1s2s2p ^{4}P metastable states (in the 10^{-6}-10^{-9} s range) of ions formed in energetic ion-atom collisions permits these to Auger decay well after their excitation in the target making it hard to determine their effective detection solid angle. Our goal is to investigate the formation mechanisms of these states through the study of their Auger decay and the determination of this solid angle is therefore of vital importance. Here, we have used the SIMION 8.1 package to treat the problem in an effective Monte Carlo type calculation. The experimental setup geometry consisting of a hemispherical deflector analyzer (HDA) with injection lens and position sensitive detector (PSD) was accurately simulated and the electrostatic potentials were determined. Random electron distributions in energy and emission angles were created simulating the metastable Auger electron decay along the path of the projectile ions, while the trajectories of the emitted electrons were traced through the HDA and counted at the PSD. A systematic study based on the above simulation procedure allowed for the accurate determination of the relevant solid angle.*

1 INTRODUCTION

Over the last few decades, considerable progress has been made in obtaining information on both the atomic structure and dynamics of multiply excited states using high resolution Auger electron spectroscopy [1,2]. This interest has been generated to a large degree in the fields of plasma physics, thermonuclear fusion research, and astrophysics where the collisional properties of highly stripped ions play an important role. The determination of highly accurate excitation energies, transition rates, and lifetimes combined with production cross section information obtained from line intensity measurements lead to a better overall understanding of the dominant processes at play.

With this goal in mind, a new experimental station for atomic collisions physics research has been developed and is currently operating at the TANDEM Accelerator of the National Research Center "Demokritos" in Athens [3]. One of the primary goals of the project is to investigate the production mechanisms of long-lived metastable 1s2s2p ^{4}P states formed in collisions of fast He-like ions with gas targets [4,5]. In more detail, we shall use a new and relatively unknown technique to isolate the production of the 1s2s2p ^{4}P and 1s2p^2 ^{2}P states arising just from the 1s2s ^{3}S component of the He-like ionic beam [6,7]. The production mechanisms will be studied by recording their Auger decay spectrum using a state-of-the-art high efficiency hemispherical electrostatic spectrometer at 0^0 to the beam direction. Our results will provide a clear systematic analysis of the intensities of ^{4}P and ^{2}P Auger lines of first row ions in an effort to resolve open issues concerning the observed non-statistical enhancement of the ^{4}P lines and the role of cascade feeding, dynamical Pauli exchange interaction and other mechanisms potentially responsible for their production [8-11].

A persistent problem in absolute cross section measurements of metastable states de-excitation arises from the inherent long lifetime of these ionic states. The ion decays all along its observation path and thus the subtended by the spectrometer solid angle varies with the variation of the decay position particularly at 0^0 observation. This fact has to be taken into to account in the analysis as it accounts for large corrections (usually factors of 5 to 10 are considered). Indeed, in the literature this problem has been treated after determining the correction factor simply geometrically. However, this method is valid only for spectrometers that do not have focusing elements at their entrance. Our spectrograph is equipped with a four-element focusing/retarding lens

that is crucial for drastically improving the resolution of the recorded spectrum, but does not allow for a straightforward treatment of the solid angle correction factor. In this report, we present a Monte Carlo approach within the SIMION simulation environment [12] to treat the problem of the accurate determination of this solid angle correction factor.

2 THE SPECTROGRAPH AND THE ASSOCIATED DDCS

The workhorse of the station is a hemispherical deflector analyzer (HDA) with a 4-element injection lens and 2-D position sensitive detector (PSD) allowing for high resolution studies of Auger electrons emitted from ions at 0^o with respect to the beam direction [13-15]. In figure 1 a general overview of the spectrograph and the electron detection process, simulated in the SIMION environment is illustrated. The ionic beam interacts with the atoms of the gas cell to continue traveling through the spectrograph to be detected at a Faraday cup. During the travel, the ions that were excited to the ^{4}P metastable state decay according to the exponential lifetime law. As a result, energetic electrons are emitted all along the path between gas cell and the HDA with variable solid angle subtending the entry of the spectrograph to be analyzed and detected at the PSD.

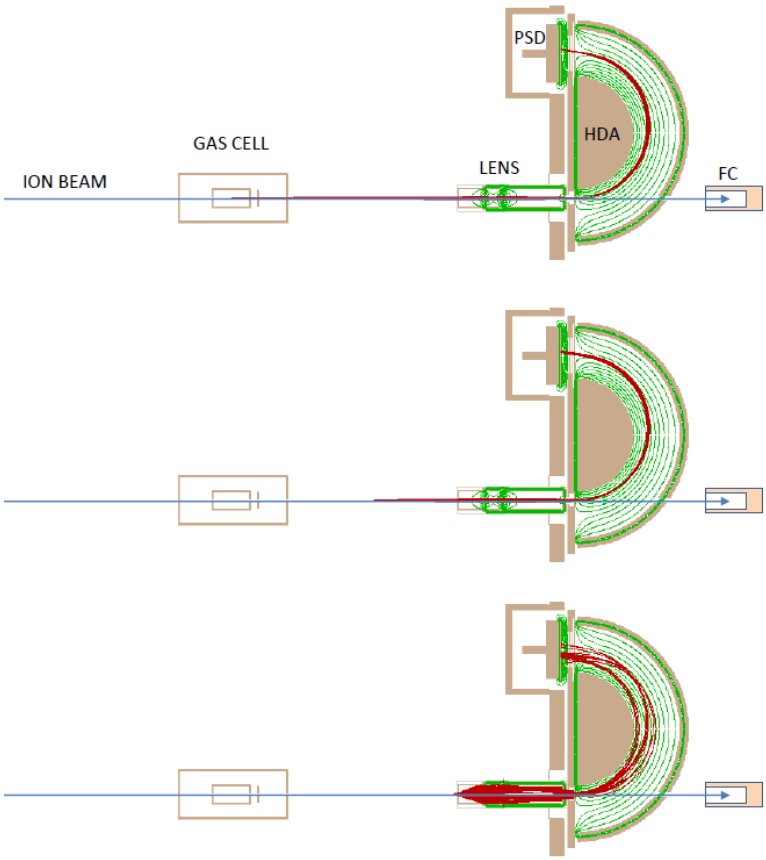

Figure 1. A two-dimensional view of the experimental setup. The ionic projectile beam interacts with the atoms at the gas cell, populating excited ionic states whose Auger decay occurs along the ions path all along to and through the spectrometer. Electrons emitted from the excited ions are focused by the lens at the entry of the HDA to be detected at the PSD at the exit of the HDA. The ions continue through the spectrometer and are collected in a Faraday cup (FC). Three different cases of the ionic states Auger de-excitation are illustrated: [*Top*] At the center of the gas cell. [*Middle*] At the mid-distance between the center of the gas cell and the lens entry. [*Bottom*] At the neighborhood of lens entry where the solid angle effects become considerable.

The measured experimental quantity in these type of measurements is the differential cross section (DCS) which for prompt states (i.e. states that decay inside the gas cell) is inversely proportional to the solid angle $\Delta\Omega$. However, in the case of the detection of long lived metastable states like the 4P, DCS has to be corrected in order to include the fact that the solid angle varies depending on the location at which the Auger decay occurred. Indeed, for ions that decay closer to the spectrograph a larger solid angle should rather be considered compared

to that of the ions that decay inside the gas cell, as it is clearly shown in figure 1 (bottom). The situation is explained in detail in section 4 after a short introduction to the kinematic effects inherent in this type of moving emitter measurements.

3 KINEMATIC CONSIDERATIONS

Auger electrons emitted from scattered projectiles are kinematically influenced. A detailed analysis of the general electron kinematic effects can be quite complicated [16]. However, for the case of energetic collisions of a few MeV/amu or larger, projectile ions are scattered through very small angles (~ mrads), resulting in a negligible effect on both the energy loss and the scattered ionic trajectories. Thus, for simplicity, the projectile ion scattering angle is typically assumed to be zero. Under this consideration, a simple velocity vector addition model is sufficient for determining the projectile-to-laboratory frame transformation and related kinematic effects, as the ion-recoil effects can be overlooked. The velocity **v** of the Auger electron in the laboratory frame is obtained by adding the projectile velocity $\mathbf{V_P}$ to the velocity **v'** of the electron in the projectile rest frame as shown in figure 2. Denoting by primed symbols the quantities in the projectile rest frame, the electron kinetic energy $\varepsilon = ½\ mv^2$ in the laboratory frame can be written in terms of the corresponding rest frame electron kinetic energy $\varepsilon = ½\ mv'^2$ and emission angle θ' as:

$$\varepsilon = \varepsilon' + t_p + 2\sqrt{\varepsilon' t_p}\cos\theta' \qquad (2)$$

where

$$t_p = \frac{1}{2}mV_p^2 = \frac{m}{M}E_p = 548.58\frac{E_p(MeV)}{M_p(amu)}eV \qquad (3)$$

is the reduced projectile energy known also as the cusp energy. E_p and M_p are the kinetic energy and mass of the projectile, respectively, while m is the electron mass.

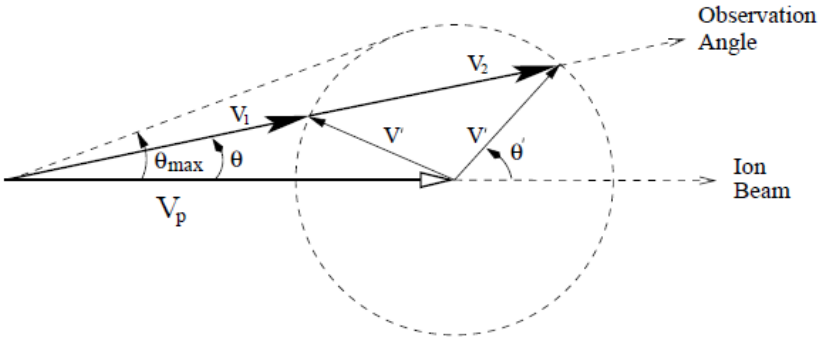

Figure 2. Velocity addition diagram. The electron velocity **v'** at the projectile rest frame is transformed at the laboratory frame according to the vector addition rule as $\mathbf{v = V_p + v'}$. Note that here the emitter velocity is larger than the electron velocity $V_p > v'$.

In order to systematically study the kinematic transformation properties of the experimentally measurable physical quantities, it is convenient to adopt the universal dimensionless parameter ζ′

$$\zeta' \equiv \sqrt{\frac{t_p}{\varepsilon'}} = \frac{V_p}{\upsilon'} \qquad (4)$$

Also it is experimentally convenient to express the relation between the energies in the laboratory frame as a function of the *laboratory* observation angle θ. Using simple trigonometric rules, geometry and the introduced parameter ζ′, the electron energy in the laboratory frame can be written as

$$\varepsilon_{\pm} = \varepsilon'\left(\zeta'\cos\theta \pm \sqrt{1-\zeta'^2\sin^2\theta}\right) \qquad (5)$$

As illustrated in figure 2, for fast emitters ($V_p > v'$, or $\zeta' > 1$) there can be two possible solutions for the

laboratory electron energy ε as a function of the laboratory detection angle θ. For fast emitters the constraint $\zeta'^2\sin^2\theta \leq 1$ results in a limitation of the available observation angle θ which can only reach a maximum value of

$$\theta_{\max} = \arcsin\frac{1}{\zeta'} \tag{6}$$

This is a crucial limitation for non-zero degree Auger Projectile Spectroscopy since different electron energies correspond to different maximum detection angles, thus setting a lower limit on the electron energies accessible to the spectrometer. However, for $\theta = 0^0$ (i.e. ZAPS technique) the whole projectile electron energy range is accessible. This is one of the most important advantages for measuring electron spectra at zero degrees.

4 THE MONTE CARLO CODE IN THE SIMION 8.1 ENVIRONMENT

SIMION 8.1 is a native Windows (Win32) ion optics simulation program that models charged particle optics problems [12]. It is designed to model electrostatic and magnetic fields and forces created by a collection of shaped electrodes given certain symmetry assumptions. The heart of SIMION strategy is the potential arrays that define the geometry of the electrodes and the potentials on these electrodes and in the empty space between them. Typically the potentials on the electrodes are defined by the user and SIMION determines the potentials in the space between the electrodes by solving the Laplace equation utilizing finite difference methods. Potential arrays are located in an ion optics workbench volume where they can be sized, oriented and positioned. Ions and electrons can be flown within the workbench volume, with their trajectories calculated from the fields inside the potential arrays instances they fly through. SIMION offers a user-friendly interface providing features that include internally defined initial particle distributions, data recording of trajectories, geometry files, and user programming with Lua.

The specific method used within SIMION to solve the boundary value problem of the Laplace equation is the finite difference technique called over-relaxation. The objective of the method is to obtain a best estimate of the potentials for the points within each potential array, a process called refining. Relaxation methods use nearest neighbor points to obtain new estimates for each point. For example, in a two-dimensional geometry the value of the potential of a point in the potential array is determined by the values of the four nearest neighbors as $V = (V_1+V_2+V_3+V_4)/4$. The process is repeated for all the points of the potential array resulting in the first iteration. Successive iterations adjust the values of the points to a predetermined accuracy. Over-relaxation method speeds up this refinement process by increasing each voltage adjustment by some factor. Relaxation techniques have the advantage that normal numerical computation errors are minimized, solutions are quite stable, and computer memory storage requirements are minimized.

The strategy in the structure of our numerical code for studying the aforementioned problem is to make use of the internally defined random sampling distribution capabilities of SIMION to create a Monte Carlo approach to the problem. Specifically, there are two factors entering the problem that need to be estimated. We shall refer to the first as *geometrical* and the second as *temporal*.

The *geometrical* factor arises from the fact that the ions decay from their excited metastable ^{4}P state throughout their travel towards and possibly through the HDA. As a result, each point of their trajectory becomes a source of Auger electrons having an acceptance solid angle determined by the entry aperture of the spectrograph and occasionally limited by kinematic considerations (i.e. θ_{max} in equation 6). Indeed, according to figure 2, electrons are emitted in the projectile rest frame in general in a 4π solid angle. However, due to the addition of velocities, in the laboratory frame electrons are confined to a maximum solid angle determined by equation 6. This fact is treated in our program by increasing the amount of generated electrons according to the ratio of the solid angle corresponding at each point $\Delta\Omega = 2\pi (1 - \cos\theta)$ to the solid angle determined by the center of the gas cell and the entry aperture of the lens of the spectrograph ($\Delta\Omega_c = 1.55\text{x}10^{-4}$ sr). Even though this geometrical factor seems to be increasing by many orders for distances very close to the aperture entry it is strongly limited by kinematics effects as described previously. Thus, for each point a number of electrons is randomly generated to be flown within the appropriate solid angle utilizing the SIMIION option of 'pupil'. For each randomly generated electron the kinetic energy of the electron is determined as follows: First a random sampling of a SIMION generated Lorentzian distribution having a central energy and a FWHM of a known Auger transition at the projectile rest frame is obtained. Then the azimuthal angle θ of the randomly generated electron is recalled from SIMION and the laboratory frame kinetic energy is calculated according to Equation 5.

The second factor is the *temporal* factor which essentially counteracts the geometrical factor. The Auger decay follows a temporal exponential decay law which for many of these transitions have been measured and/or calculated. Thus, typically the decay law $N(t) = N_i \exp(-t/\tau)$ is adopted. N_i is the initial number of electrons (at

t=0) and τ is the lifetime of the Auger transition. The variable t is simply the time-of-flight of the ion determined by the kinetic energy of the ion beam. We should point out here that the electrons are generated randomly in the cylindrical volume of the gas cell in the path of the ion beam as it goes through the gas cell. The same cylindrical geometry is maintained for the electron generation during the passage of the ion beam outside the gas cell all the way through the spectrograph.

Based on the above analysis, for each point along the ion trajectory a number of electrons is created to be flown towards the spectrograph which is the product of three numbers: i) the starting number of electrons at the centre of the gas cell N_i, ii) the geometrical factor $f_G = \Delta\Omega/ \Delta\Omega_c$ and iii) the temporal factor $f_T = \exp(-t/\tau)$. The final correction results after dividing the number of particles that are detected on the PSD within the limits of the Auger line energy distribution to the number of particles N_i.

5 RESULTS AND DISCUSSION

In figure 3 we present the simulation results of the detection of the $1s2s2p\ ^4P_{3/2}$ metastable state, formed in collisions of 40 MeV $F^{7+}(1s2s) + H_2$, Auger decaying to the ground state of $F^{7+}(1s^2)$ with a lifetime of $\tau = 1.84$ ns emitting an electron with a projectile frame rest energy of $\varepsilon' = 528$ eV. The electrons that meet the condition for emittance very close to zero-degrees with respect to the ion beam are detected at the center of the PSD. According to kinematic considerations the electrons appear to have a central kinetic energy in the laboratory frame of 3256 eV which is clearly shown in figure 3. Electrons that do not meet the above conditions are not detected as they hit either the walls of the lens and/or the HDA. These electrons were rejected due to their large solid angle departing from zero degrees resulting also in kinematically altered kinetic energies (see equation 5). Both these effects result in inappropriate conditions for lens focusing and further transmission through the HDA and on to final counting by the detector.

In figure 3 the metastable state is depicted with a red solid line while the same state decaying as prompt state is depicted with a blue dash-dotted line. Essentially the prompt state corresponds to the emission of electrons from the center of the gas cell after omitting all the temporal decay and the corresponding geometrical solid angle summations. Thus, the corrections factor results as the division of the areas of the two peaks which in this case turns out to be 1.6

Based on these simulations it becomes clear that the role of the lens is twofold. First of all, the lens focuses all electrons at the entry of the HDA primarily those with paraxial trajectories. All electrons that deviate from the paraxial rays largely depart from the central ray neighborhood and hit the walls of the lens or the walls of the entry HDA aperture. For those that make it through the HDA aperture, they have large entry angles resulting in detection at the PSD but outside of the proper range of the peak and thus are detected as background. The situation is even worse for electrons generated at quite larger angles θ since their energy in the laboratory frame deviates from the central energy to which the HDA and the lens have been tuned. Thus, their rejection primarily by the lens is almost certain. Second, the lens acts as a filter for the majority of the electrons that are generated inside the lens independent on their trajectories. The reason is that these electrons will have an altered kinetic energy by the amount of the value of voltage at the point of birth. Therefore their kinetic energy will be out of the acceptance energy window of the lens and the HDA and consequently they will not be detected at all or in the worst case will be detected as a background signal somewhere on the PSD.

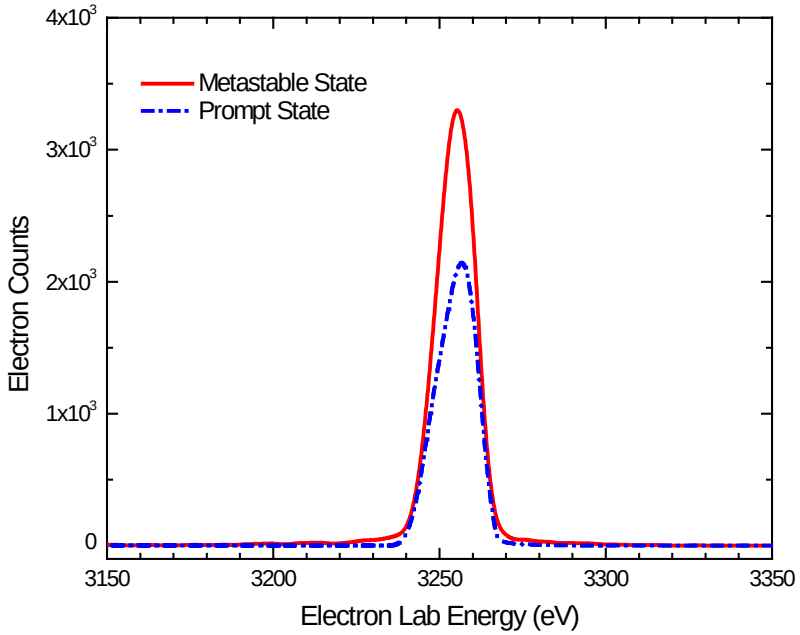

Figure 3. SIMION8.1 results concerning the determination of the solid angle correction factor. See text for details.

We should point out here that in the literature similar problems have been treated after determining the two factors simply geometrically without the help of the SIMION or some other simulation program. However, as earlier mentioned, these approaches are correct only because they refer to spectrometers that do not have focusing elements at their entrance. Our spectrograph is equipped with a four-element focusing/retarding lens that is crucial for drastically improving the resolution of the spectrograph but does not allow for a straightforward treatment of the two factors. At this point the Monte Carlo treatment within the SIMION environment seems a viable way to study the problem

6 CONCLUSIONS

In the present work, we used an effective Monte Carlo type calculation to treat the problem of the determination of the effective detection solid angle for the Auger decay of metastable states formed in energetic ion-atom collisions. We simulated the experimental setup geometry in the SIMION 8.1 ion simulation package and accurately reproduced the experimental conditions. Thus, we were able to demonstrate in a proof-of-principle calculation the procedure for the determination of the correction factor in the effective solid angle for the $1s2s2p\ ^4P_{1/2}$ metastable state, formed in collisions of 40 MeV $F^{7+}(1s2s) + H_2$, decaying to the ground state of F^{7+} $(1s^2)$.

ACKNOWLEDGEMENT

Co-financed by the European Union (European Social Fund—ESF) and Greek national funds through the Operational Program "Education and Lifelong Learning" of the National Strategic Reference Framework (NSRF)—Research Funding Program: THALES. Investing in knowledge society through the European Social Fund (Grant No. MIS 377289)

REFERENCES

[1] Zouros, T.J.M. and Lee, D.H., (1997), *Zero-degree Auger electron spectroscopy of projectile ions*, in Accelerator–Based Atomic Physics Techniques and Applications, edited by S.M. Shafroth and J.C. Austin, (AIP, NY, 1997), chapter 13, pp. 427-479.

[2] Stolterfoht, N., DuBois, R.D. and Rivarola, RD (1997), *Electron emission in heavy ion-atom collisions*, Springer-Verlag, Berlin.

[3] http://apapes.physics.uoc.gr

[4] Zouros, T.J.M., Benis, E.P. and Gorczyca, T.W. (2003), "Large-angle elastic resonant and non-resonant scattering of electrons from $B^{3+}(1s^2)$ and $B^{4+}(1s)$ ions: Comparison of experiment and theory", Phys. Rev. A, Vol. 68, pp. 010701(R).

[5] Benis, E.P., Zouros, T.J.M., Gorczyca, T.W., Gonzalez, A.D. and Richard P. (2006), "Elastic resonant and non-resonant scattering of quasi-free electrons on $B^{4+}(1s)$ and $B^{3+}(1s^2)$ ions", Phys. Rev. A, Vol. 69, pp. 052718; Erratum: ibid Vol. 73, pp. 029901E.

[6] Benis, E.P., Zamkov, M., Richard, P. and Zouros, T.J.M. (2002) "Technique for the determination of the 1s2s ^{3}S metastable fraction in two-electron ion beams", Phys. Rev. A, Vol. 65, pp. 064701.

[7] Benis, E.P., Zamkov, M., Richard, P. and Zouros, T.J.M. (2003), "Comparison of two experimental techniques for the determination of the 1s2s ^{3}S metastable beam fraction in energetic B^{3+} ions", Nucl. Instr. & Meth. in Phys. Res. B 205, 517-521.

[8] Tanis, J.A., Landers, A.L., Pole, D.J., Alnaser, A.S., Hossain, S. and Kirchner, T. (2004), "Evidence for Pauli exchange leading to excited-state enhancement in electron transfer", Phys. Rev. Lett., Vol. 92, pp. 133201; Erratum: ibid. (2006), Vol. 96, pp. 019901E.

[9] Zouros, T.J.M., Sulik, B., Gulyas, L. and Tokesi, K (2008), "Selective enhancement of 1s2s2p ^4P_J metastable states populated by cascades in single electron transfer collisions of $F^{7+}(1s^2$-1s2s ^{3}S) ions with He and H_2 targets", Phys. Rev. A, Vol. 77, pp. 050701R .

[10] Strohschein, D., Röhrbein, D., Kirchner, T., Fritzsche, S., Baran, J. and Tanis, J.A. (2008), "Nonstatistical enhancement of the 1s2s2p 4P state in electron transfer in 0.5–1.0-MeV/u $C^{4,5}$+ He and Ne collisions", Phys. Rev. A, Vol. 77, pp. 022706.

[11] Rohrbein, D., Kirchner, T. and Fritsche, S. (2010), "Role of cascade and Auger effects in the enhanced population of the C^{3+}(1s2s2p ^{4}P) states following single-electron capture in C^{4+}(1s2s ^{3}S)-He collisions", Phys. Rev. A, Vol. 81, pp. 042701.

[12] http://simion.com

[13] Benis, E.P. and Zouros, T.J.M. (2000), "Improving the energy resolution of a hemispherical spectrograph using a paracentric entry at a non-zero potential", Nuclear Instrum. & Meth. Phys. Res. A., Letter to the editor, Vol. 440, pp. 462-5.

[14] Zouros, T.J.M. and Benis, E.P. (2002) "The hemispherical deflector analyzer revisited: I. Generalized entry conditions, Kepler orbits and spectrometer basic equation", Invited Review, J. Electron Spectroscopy & Related Phenomena, Vol. 125, pp. 221-248. Erratum: ibid. Vol. 142, pp. 175–176.

[15] Benis, E.P. and Zouros, T.J.M. (2008), "The hemispherical deflector analyzer revisited: II. Electron-optical properties", J. Electron Spectroscopy & Related Phenomena, Vol. 163, pp. 28-39.

[16] Stolterfoht, N. (1987), "High resolution Auger spectroscopy in energetic ion atom collisions", Physics Reports, Vol. 146, pp. 315-424.